Charge Sensitivity/Bond-Order Analysis of Reactivity Trends in Allyl−[MoO_3] Chemisorption Systems: A Comparison between (010) and (100) Surfaces

R. F. Nalewajski*

K. Gumiński Department of Theoretical Chemistry, Jagiellonian University, R. Ingardena 3, 30-060 Cracow, Poland

A. Michalak

Department of Computational Methods in Chemistry, Jagiellonian University, R. Ingardena 3, 30-060 Cracow, Poland

Received: August 6, 1997[⊗]

In a search for the molecular mechanism of the selective oxidation of allyl to acrolein on a MoO_3 surface the previously reported charge responses and bond multiplicities for the allyl−[(010)-MoO_3] chemisorption system are compared with the corresponding results for selected allyl−[(100)-MoO_3] structures. The *charge sensitivity analysis* (CSA) in atomic resolution is used to predict the displacements in atomic electron populations for large clusters at both the *polarization* (P) and *charge transfer* (CT) stages. The changes in effective bond orders, generated for small surface clusters, are from the Kohn−Sham (LSDA) difference approach. In contrast to the energetically most favorable "perpendicular" adsorption arrangements of allyl on a smooth (010)-MoO_3 surface, the "parallel" orientation of allyl on the rough (100)-MoO_3 surface is preferred energetically. It is found that the total (P + CT) CSA charge responses due to adsorption are strongly CT-dominated (chemisorption) in the vertical structures; they are practically of P character (physisorption) in the horizontal complexes. The quantum mechanical bond-order analysis reveals a specific bond-forming−bond-weakening mechanism of substituting the terminal hydrogen of allyl by the singly coordinated lattice oxygen in the perpendicular complexes. A nonspecific bond weakening inside the adsorbate, accompanied by an overall bonding between the allyl π-electrons and the molybdenum atom, is revealed in the parallel complexes. These observations are in good agreement with the experimentally determined activity of the (010) surface and inacivity of the (100) cut of the MoO_3 crystal in catalyzing the selective oxidation of allyl to acrolein.

1. Introduction

One of the primary goals of theoretical chemistry is to identify main factors influencing chemical reactivity and to formulate/rationalize molecular mechanisms of elementary processes.[1−5] A fast development of quantum chemistry codes, particularly of the *density functional theory* (DFT)[3,6−11] and related physical models[4] that are applicable to large molecular systems, allows one to explore reactivity trends of realistic, model chemisorption systems.[4,11−13] A recent example of such an analysis is the charge sensitivity and bond-order study of the allyl−[(010)-MoO_3] chemisorption system[14] undertaken to rationalize the experimentally determined catalytic activity of this relatively smooth crystallographic face (see Figure 1c) in the selective oxidation of allyl to acrolein, an intermediate step in the selective oxidation of propylene.[15] The rough (100) cut (see Figure 1a) has been found to be practically inactive in this elementary reaction.[15] To rationalize a strong activity of the (010) surface and the high selectivity of this catalytic process, this recent model study[14] has proposed a specific concerted bond-breaking−bond-forming mechanism of replacing the terminal allyl hydrogen by the singly coordinated lattice oxygen in the energetically preferred "perpendicular" adsorption of allyl on the surface. This mechanism has been conjectured from both the charge displacement patterns determined from the two-reactant *charge sensitivity analysis* (CSA) in atomic resolution,[4,13,14,18] performed on a relatively large, two-layer cluster representation of the surface (Figure 1c), and the *Kohn−Sham* (KS) energies and quantum mechanical bond multiplicities (from the difference approach),[14,16,17] calculated for small active-site clusters (Figure 1d).

To complete this analysis, we report in the present work the corresponding results for the chemisorption systems involving the *inactive* (100) surface. It is our goal to compare the main trends exhibited by the charge displacements and changes in the bond orders due to adsorption, in the selected chemisorption complexes involving these two surfaces, with the purpose of identifying the manifestations of the catalytic activity of the (010) face and the inactivity of the (100) cut in this specific oxidation reaction. It is expected that such an analysis will deepen our physical understanding of this particular catalytic system.

2. Calculations

The same theoretical models and numerical techniques as those used in the previous study[14] have been adopted in the present work. They include the two-reactant CSA treatment in atomic resolution of chemisorption systems [4,13,14,18] and the one-determinant (KS) difference approach to bond multiplicities.[14,16,17] The CSA linear charge responses, at the *polarization* (P, physisorption), *charge transfer* (CT, chemisorption), and

[⊗] Abstract published in *Advance ACS Abstracts,* December 15, 1997.

S1089-5639(97)02566-8 CCC: $15.00 © 1998 American Chemical Society
Published on Web 01/15/1998

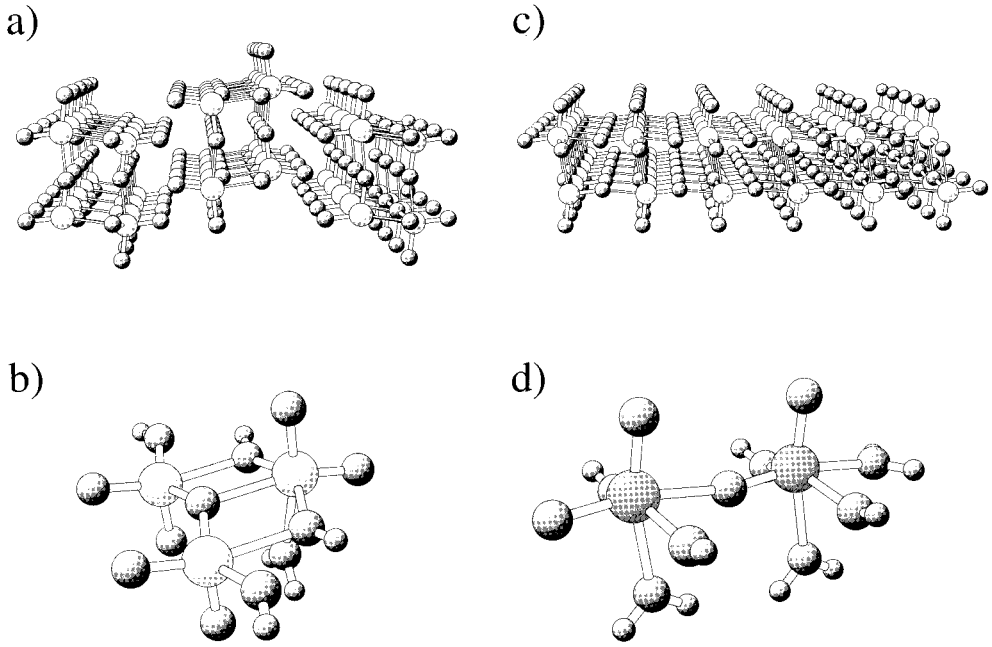

Figure 1. Cluster models of the (100)-MoO_3 (panels a and b) and (010)-MoO_3 (panels c and d) surfaces. The large clusters, $Mo_{54}O_{162}$ (panel a) and $Mo_{66}O_{198}$ (panel c), represent the two-layer models used in the CSA calculations; larger spheres denote the molybdenum atoms. The small clusters, $Mo_3O_{12}H_6$ (panel b) and $Mo_2O_{11}H_{10}$ (panel d), have been used in the KS (LSDA) calculations; the hydrogen atoms, represented by the smallest spheres in panels b and d, saturate the dangling bonds on the cluster lattice oxygens. The crystallographic bond lengths and angles have been used.

overall (P + CT) levels, are determined from the semiempirical finite difference chemical potentials of atoms and the hardness matrix of the whole chemisorption cluster, reflecting the electron−electron repulsion between the valence electrons of constituent atoms. The point-charge electrostatic potential values of one reactant at positions of nuclei of the other reactant have been used to represent the external potential perturbation data.[4,13,14] Both diagonal and off-diagonal components of the Fukui and linear response functions in atomic resolution are included in the consistent two-reactant approach.[4,18] The crystallographic values of bond lengths and angles in the MoO_3 crystal[19] and the previously reported[14] atomic charges from the ZINDO calculations for the large MoO_3 clusters and allyl have been used to generate the canonical hardness matrix and the perturbing atomic external potential data. As before, the large cluster charges have been obtained by translationally propagating charges of a few crystallographically distinct sites obtained from the ZINDO calculations on the medium-sized $Mo_{20}O_{68}H_{16}$ cluster. The frozen allyl geometry (ZINDO optimized) was used in all chemisorption complexes compared in the present work.

Following the recent bond-order analysis,[17] we have changed the signs of all bond multiplicities defined previously[14,16] so that the absolute bond multiplicities are always positive, in agreement with chemical intuition. Therefore, in contrast to the previous work,[14] the *positive* (*negative*) bond-multiplicity displacements stand for the *increase* (*decrease*) of the bond orders in question.

Figure 1 shows the perspective views of the large and small cluster representations of both (100)- and (010)-MoO_3 surfaces. To compensate for the missing crystal environment of the small clusters used in the KS calculations, the standard saturation[20] of dangling bonds by hydrogens have also been applied in this study.

The (100)-surface chemisorption arrangements of Figures 2 and 3 include two "perpendicular" adsorptions of allyl above the lattice oxygens (structures in parts a and b) and two "parallel" adsorptions of allyl above the molybdenum atom (structures in parts c and d). For comparison, also reported are the results corresponding to the "perpendicular" adsorption complex (structure in part e of Figures 2 and 3) on the (010)-surface, which has been previously recognized as the crucial structure explaining the smooth surface reactivity and selectivity. The two perpendicular geometries on the (100)-surface have the same allyl−surface separation as that in the reference structure of part e of Figures 2 and 3. They exhibit the same arrangement of the terminal methylene group of allyl relative to the active-site oxygens. The parallel geometries correspond to roughly the same value of the shortest C−O distance, as in the case of the reference geometry in part e of Figures 2 and 3. This criterion has been selected owing to the conjectured importance of the substitution of the terminal hydrogen by the lattice oxygen for the molecular mechanism of acrolein formation.[14] Throughout the paper atomic units are used. In the charge response diagrams of Figure 2 the black (white) circles denote the negative (positive) electron population displacements, the magnitude of which is reflected by the circle areas.

3. Results and Discussion

In Figure 2 the CSA diagrams of charge displacements due to adsorption are presented for the four chemisorption structures involving large (100)-surface cluster and the reference (reactive) perpendicular complex including the large (010)-surface cluster. The total (P + CT) changes are resolved into the corresponding P and CT contributions. The former reflects the internal polarizations inside the allyl and the surface due to the external potential perturbation of the other reactant. The latter shows the effect of the subsequent CT. In all cases the spontaneous allyl → surface CT direction has been predicted, as shown by the arrows in the figure. The CSA and KS estimates of the equilibrium amount of CT (N_{CT}) and the CSA energy changes due to adsorption at the *electrostatic* (ES), P, and CT stages are reported in Table 1 together with the corresponding total KS energy changes for small chemisorption clusters. The CSA

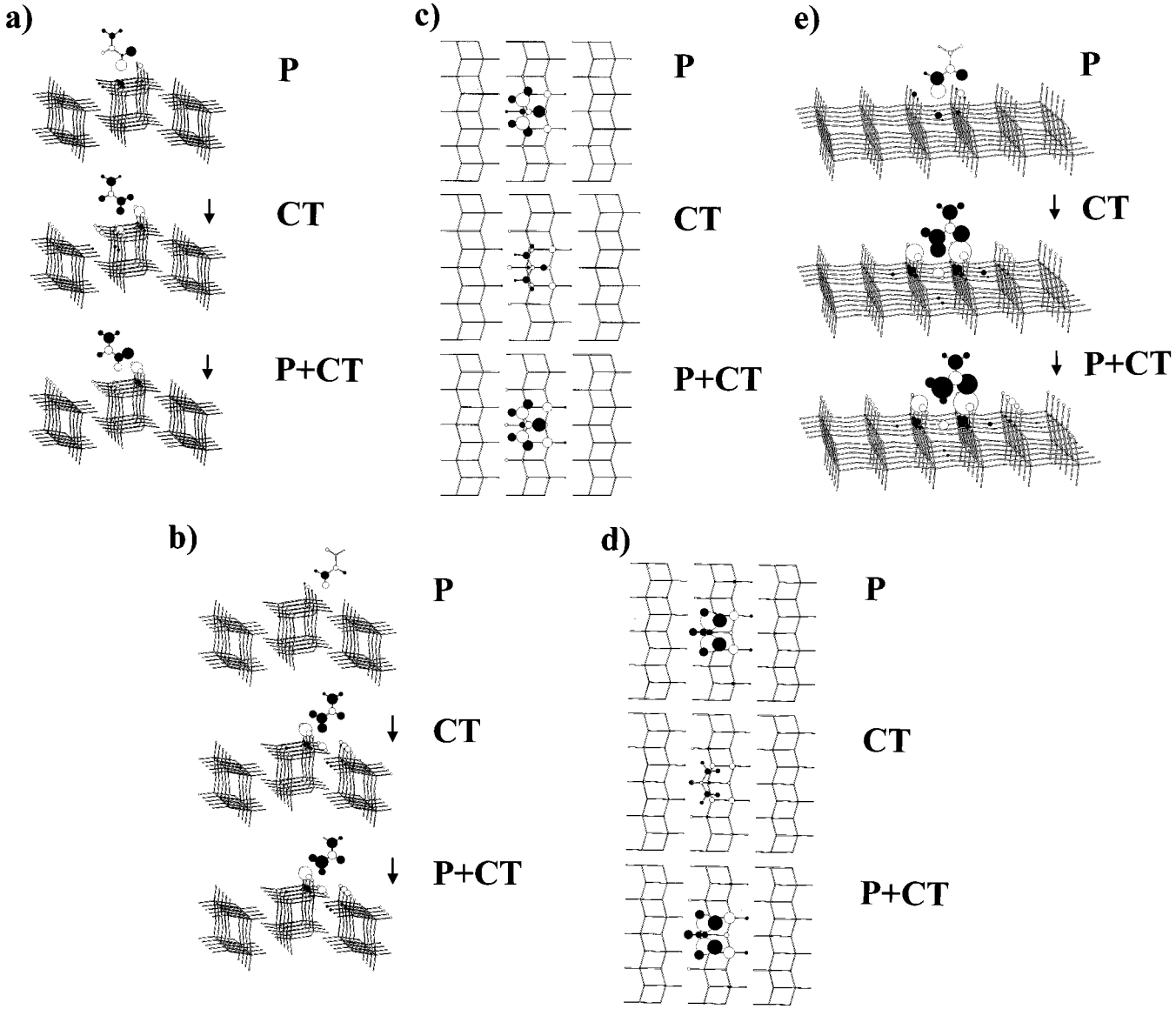

Figure 2. P, CT, and (P + CT) diagrams for the four allyl−[(100)-MoO_3] chemisorption complexes (panels a−d) and the reference allyl−[(010)-MoO_3] structure (panel e). To facilitate a comparison, a common value of the scale factor has been adopted in all diagrams.

electrostatic contribution corresponds to the "frozen" charges of constituent atoms in isolated reactants.

The main total (ionic + covalent) shifts of the bond multiplicities due to adsorption, as predicted by the difference approach, are listed in Figure 3; the cutoff magnitude is 0.01. In all arrangements the covalent contribution strongly dominates the total bond-order displacement. The largest ionic contributions, on the order of 20−30%, have been observed in the active-site region of the surface and the strongest allyl−surface bonds. Inside the allyl, particularly in the parallel complexes, the ionic contribution is generally less than 10% of the total value.

A general feature of the total charge redistribution diagrams of Figure 2 is their remarkable localization in the chemisorption, first-layer region. This is also true in the case of all the P and CT diagrams. This fast decay of the chemisorption disturbance inside the oxide surface a posteriori validates the cluster representation selected in this study. It also shows that even smaller clusters, e.g., of the order of those used in KS calculations [parts b and d of Figure 1], cover most of the active-site region determined by atoms undergoing the largest population shifts. We would like to emphasize, however, that a larger portion of a crystal surface is required to realistically simulate the Madelung potential on the active-site region. This localized character of the chemisorption charge rearrangement is also independently reflected by the KS bond-multiplicity changes reported in Figure 3.

It follows from a comparison of the (P + CT) panels in Figure 2 that all four (100)-surface complexes (parts a−d) generate much smaller charge displacements than the reactive (010)-surface complex (part e). An examination of their resolutions into the P and CT parts further reveals that in parallel arrangements (parts c and d) the polarization components strongly dominate over the corresponding CT contributions. This is not the case in the perpendicular geometries (parts a, b, and e), where P and CT components are of comparable magnitude. This is also reflected by the N_{CT} data of Table 1, where the smallest values are found in the horizontal arrangements of allyl. Therefore, one would generally conclude from these charge rearrangement diagrams that the parallel adsorption bond is of mainly physisorption character, while that in all perpendicular cases has also a strong CT (chemisorption) origin.

A more detailed survey of the charge displacement patterns inside allyl in all vertical complexes (parts a, b, and e) indicates that to a large degree they resemble one another. This implies

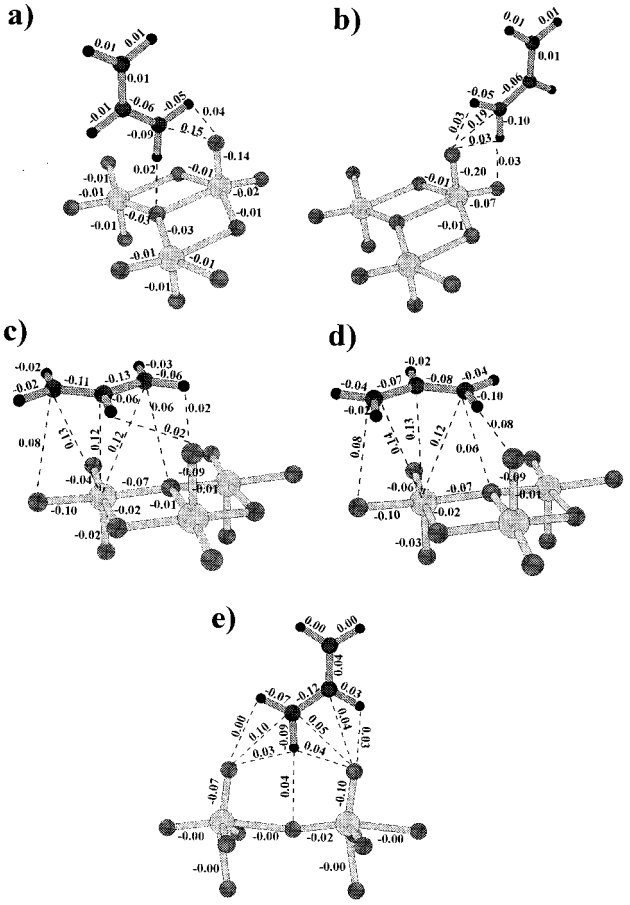

Figure 3. Patterns of the bond-multiplicity changes due to adsorption, from the one-determinant (KS) difference approach, for the five adsorption arrangements of Figure 2.

TABLE 1: CSA and KS Interaction Energies (au) and the Amounts of the Allyl → Cluster CT, N_{CT}, for the Chemisorption Complexes of Parts a−e of Figure 2

	complex				
	a	b	c	d	e
			CSA		
energies					
ES	−0.0001	0.0002	−0.0023	−0.0031	0.0002
P	−0.0029	−0.0002	−0.0023	−0.0040	−0.0019
ES + P	−0.0030	0.0000	−0.0045	−0.0071	−0.0016
CT	−0.0045	−0.0172	−0.0016	−0.0016	−0.0356
ES + P + CT	−0.0076	−0.0172	−0.0061	−0.0086	−0.0372
N_{CT}	0.26	0.51	0.18	0.17	0.83
			KS		
ΔE	−0.0011	0.0091	−0.0280	−0.0246	−0.0103
N_{CT}	0.12	0.10	0.19	0.17	0.05

a qualitative similarity of the related patterns of shifts in the bond multiplicities, as indeed detected in Figure 3. One also observes the same positive electron population change on the terminal, singly coordinated lattice oxygen, forming a partial bond with the allyl carbon atom, in all perpendicular chemisorption arrangements.

A major difference between the perpendicular (100)- and (010)-surface complexes is the presence of an additional lattice oxygen in the latter case, also singly coordinated, which "anchors" the middle carbon hydrogen. This feature can be expected to be important for the concerted atom exchange mechanism on the terminal carbon, toward acrolein,[14] since it effectively binds the adsorbate when another surface bond (Mo−O) is weakened as a result of the atom exchange. Indeed, this anchoring molybdenyl oxygen atom exhibits the largest positive displacement in the total diagram of Figure 2e. The geometric arrangement of the active site on the (100)-surface is different, providing for no such an anchoring possibility. Yet another general difference between the perpendicular complexes on the two crystallographic faces is that the surface charge reconstruction is visibly smaller in the rough (100)-case.

The total charge rearrangements in the vertically and horizontally adsorbed allyl on the (100)-surface exhibit notable differences inside the carbon chain. Namely, the electrons are predicted to be removed from the terminal carbons in the perpendicular geometries, while the opposite pattern is observed in the parallel complexes. A reference to the bond-order diagrams of Figure 3 shows that the C−C bonds are in general symmetrically weakened in the parallel complexes, while a strong asymmetric pattern is found for the perpendicular complexes, with the bond more distant from the surface being slightly strengthened as is the case in acrolein.

The qualitative trends exhibited by the total (P + CT) CSA pattern of Figure 2a compare favorably with those reflected by the charge displacement data from the KS calculations on a small cluster. A similar conclusion follows from the corresponding examination of the CSA and KS charge displacements for the complex of Figure 2b. The only exception in this case is the terminal hydrogen strongly interacting with the two molybdenyl oxygens, which in the KS pattern slightly accumulates electrons, relative to the separated allyl charge distribution. This difference is due to a relatively large N_{CT} value predicted within the CSA for this complex, 5 times as large as the amount predicted by the DFT calculations. In the complex of Figure 2c, the total equilibrium charge transfers from both calculations are almost identical; the main components of the corresponding total charge displacement diagrams are indeed very similar in the CSA and KS approaches, although the charge displacements on carbons are practically vanishing in the KS approximation. This qualitative difference in the predicted polarization of the carbon chain is due to the inability of the (*symmetric*) atomic resolution model to describe the polarization of atoms themselves. Such charge distortion must strongly contribute to the polarization of the π-electrons in the two parallel arrangements. The same qualitative difference in the CSA and KS polarizations of the carbon chain is observed for the complex of Figure 2d. Indeed, the CSA pattern agrees with the KS one for all atoms except the carbons. Finally, for the previously reported reference structure in Figure 2e, the KS charge redistribution inside allyl resembles more the CSA P-pattern than the total one. Actually, the N_{CT} values of Table 1 are dramatically different in both approaches, with the LSDA calculations predicting only a small contribution from the CT component. At this point one should recall that the Mulliken population analysis of the KS scheme may be very misleading in calculations using quite extended basis sets including polarization functions, e.g., the DZVP basis set used in the present study.

Let us now examine in more detail the KS bond-multiplicity diagrams of Figure 3, focusing on the adsorbate−surface bond orders and those reflecting the surface reconstruction due to adsorption. The first general observation is that in all structures the active-site molybdenyl bonds, including oxygens that strongly interact with allyl, are substantially weakened. The bridging oxygen bonds are seen to be less affected by the perpendicular adsorption of allyl. In the parallel adsorption arrangements above the molybdenum site there is a strong bond-

weakening effect observed in two Mo−O bonds at the base of the adsorption site pyramid, leading to its eventual distortion.

The strongest adsorption bonds in the perpendicular structures of panels a and b are between the terminal carbon of allyl and the terminal oxygen of the surface. In the reference structure of part e this effect is distinctly weaker, although in this case the carbon effectively forms partial bonds with two terminal oxygens. Therefore, the overall O−C−O bond multiplicity in the complex of part e is of comparable magnitude to the C−O bond in structures in parts a and b. A qualitatively different picture emerges from the parallel panels c and d. Namely, the chemisorption bonds between all three carbon atoms and the Mo adsorption site are similar and much stronger then the corresponding C−O bonds, the latter being crucial for the selective oxidation of allyl. Therefore, only the vertical adsorption complexes can account for a possible selective oxidation of allyl to acrolein, with the horizontal complexes eventually leading to a total destruction (nonselective oxidation) of the adsorbate.

Clearly, it is the total adsorption energy that discriminates between these two mechanisms on the surface in question. On the (010)-surface, mainly owing to the electrostatic factors, the perpendicular adsorption is strongly favored; the DFT adsorption energies of Table 1 show that on the (100)-surface the parallel adsorption is preferred. This provides a sound physical explanation of the experimentally observed differences in catalytic activity of the two MoO_3 crystallographic cuts.

Finally, let us comment upon the CSA energy estimates reported in Table 1. It follows from the ES data that the parallel complexes are also electrostatically preferred on the (100)-surface. The same is true at the (ES + P) approximation level. However, owing to the exceptionally large N_{CT} value predicted for the structure in part b, it becomes the most favored by the (ES + P + CT) energy estimate. We remark, however, that the CSA classical energy does not include the important exchange contribution, which could substantially affect the total adsorption energy, particularly at such a close adsorbate−substrate separation.

4. Conclusion

This type of the charge-sensitivity/bond-multiplicity analysis of chemisorption systems, combining the exact LSDA calculations on small clusters with the CSA charge redistribution patterns on large clusters, has been demonstrated to be a useful probing tool that allows one to diagnose both reactive and nonreactive systems. The two approaches complement each other: the former generates a reliable energetical hierarchy of admissible chemisorption geometries and the corresponding bond activation/reconstruction diagrams, while the latter predicts realistic charge displacement patterns in atomic resolution in quite a realistic representation of the active site environment in the crystal.

A comparison between the allyl chemisorption systems on the (010)- and (100)-MoO_3 surfaces demonstrates that the former catalyzes the selective oxidation of the adsorbate to acrolein because the perpendicular adsorption is preferred; the latter surface exhibits a strong preference for the parallel allyl adsorption, for which the related patterns of charge displacements and bond activations do not imply such selectivity. The P vs CT resolution of the overall CSA charge displacements predicts the physisorption-dominated bond in the parallel adsorption complexes on the (100)-surface, while in all perpendicular structures a strong CT component is determined.

Acknowledgment. This work was partly supported by a research grant from the State Committee for Scientific Research in Poland (Project T09A 046 12). One of the authors (A.M.) also acknowledges the support via the Fellowship for Young Scientists from the Foundation for Polish Science.

References and Notes

(1) Fukui, K. *Theory of Orientation and Stereoselection*; Springer-Verlag: Berlin, 1982.

(2) Bader, R. F. W. *Atoms in Molecules: A Quantum Theory*; Clarendon Press: Oxford, 1990.

(3) Parr, R. G.; Yang, W. *Density Functional Theory of Atoms and Molecules*; Oxford University Press: New York, 1989.

(4) Nalewajski, R. F.; Korchowiec, J. *Charge Sensitivity Approach to Molecular Structure and Chemical Reactivity*; World Scientific: Singapore, 1997.

(5) Nalewajski, R. F., Ed. Theory of Chemical Reactivity. In *Density Functional Theory*; Topics in Current Chemistry 183; Springer-Verlag: Heidelberg, 1996.

(6) Hohenberg, P.; Kohn, W. *Phys. Rev.* **1964**, *B136*, 864. Kohn, W.; Sham, L. J. *Phys. Rev.* **1965**, *A140*, 1133.

(7) Dreizler, R. M.; Gross, E. K. U. *Density Functional Theory: an Approach to the Quantum Many-Body Problem*; Springer-Verlag: Berlin, 1990.

(8) Gross, E. K. U., Dreizler, R. M., Eds. *Proceedings of the NATO ASI on Density Functional Theory*, Il Ciocco, August 16−27, 1993; Plenum Press: New York, 1995.

(9) Nalewajski, R. F., Ed. *Density Functional Theory*; Topics in Current Chemistry 180−183; Springer-Verlag: Heidelberg, 1996.

(10) Yang, W. *Phys. Rev. Lett.* **1991**, *66*, 1438. Yang, W.; Lee, T. *J. Chem. Phys.* **1995**, *103*, 5674. Zhu, T.; Pan, W.; Yang, W. *Phys. Rev. B* **1996**, *53*, 12713. Lee, T.; York, D.; Yang, W. *J. Chem. Phys.* **1996**, *105*, 2744.

(11) Salahub, D. R., Russo, N., Eds. *Proceedings of the NATO ASI on Metal-Ligand Interactions: From Atoms, to Clusters, to Surfaces*, Cetraro, June 10−21, 1991; Kluwer Academic Publishers: Dordrecht, 1992.

(12) Schoonheydt, R., Ed. *Trends in Physical Chemistry: The Activated Complex in Heterogeneous Catalysis*; Research Signpost, in press.

(13) Nalewajski, R. F.; Korchowiec, J. *J. Mol. Catal. A* **1996**, *112*, 167.

(14) Nalewajski, R. F.; Michalak A. *J. Phys. Chem.* **1996**, *100*, 20076.

(15) Grzybowska, B.; Haber, J.; Janas, J. *J. Catal.* **1977,** *49*, 150. Brückman, K.; Haber, J.; Wiltowski, T. *J. Catal.* **1987**, *106*, 188. Brückman, K.; Grabowski, R.; Haber, J.; Mazurkiewicz, A.; Słoczyński, J.; Wiltowski, T. *J. Catal.* **1987**, *104*, 71. Bielański A.; Haber J. *Oxygen in Catalysis*; Marcell Dekker: New York, 1991. Haber, J. In *Molybdenum: An Outline of its Chemistry and Uses*; Braithwaite, E. R., Haber J., Eds.; Elsevier: Amsterdam, 1994.

(16) Nalewajski, R. F.; Mrozek, J. *Int. J. Quantum Chem.* **1994**, *51*, 187. Nalewajski, R. F.; Formosinho, S. J.; Varandas, A. J. C.; Mrozek, J. *Int J Quantum Chem* **1994**, *52*, 1153. Nalewajski, R. F.; Mrozek, J.; Mazur, G. *Can. J. Chem.* **1996**, *74*, 1121. Nalewajski, R. F.; Mrozek, J.; Michalak, A. *Int. J. Quantum Chem.* **1997**, *61*, 589.

(17) Mrozek, J.; Nalewajski, R. F.; Michalak, A. *Pol. J. Chem.*, in press.

(18) Nalewajski, R. F.; Korchowiec, J.; Michalak, A. Theory of Chemical Reactivity. In *Density Functional Theory*; Nalewajski, R. F., Ed.; Topics in Current Chemistry 183; Springer-Verlag: Heidelberg, 1996; p 25. Nalewajski, R. F. In *Trends in Physical Chemistry: The Activated Complex in Heterogeneous Catalysis*; Schoonheydt, R., Ed.; Research Signpost, in press.

(19) Kihlborg, L. *Ark. Kemi* **1963**, *21*, 357.

(20) Michalak, A.; Hermann, K.; Witko, M. *Surf. Sci.* **1996**, *366*, 323.